

# Nonreciprocal Perfect Coulomb Drag in Electron–Hole Bilayers: Coherent Exciton Superflow as a Diode

Jun-Xiao Hui (辉隽骁)<sup>1</sup>, Qing-Dong Jiang (蒋庆东)<sup>1,2\*</sup>

<sup>1</sup> Tsung-Dao Lee Institute & School of Physics and Astronomy,

Shanghai Jiao Tong University, Pudong, Shanghai, 201210, China

<sup>2</sup> Shanghai Branch, Hefei National Laboratory, Shanghai, 201315, China.

Distinguishing an exciton condensate from an excitonic gas or insulator remains a fundamental challenge, as both phases feature bound electron–hole pairs but differ only by the emergence of macroscopic phase coherence. Here, we theoretically propose that a spin–orbit–coupled bilayer system can host a finite-momentum exciton condensate exhibiting a nonreciprocal perfect Coulomb drag—the *coherent-exciton diode effect*. This effect arises from the simultaneous breaking of inversion and time-reversal symmetries in the exciton condensate, resulting in direction-dependent critical counterflow currents. The resulting nonreciprocal perfect Coulomb drag provides a clear and unambiguous transport signature of phase-coherent exciton condensation, offering a powerful and experimentally accessible approach to identify, probe, and control exciton superfluidity in solid-state platforms.

*Introduction.*—Excitons, first proposed by Frenkel [1] to explain the light absorption of solids, are bound states of an electron and a hole that appear widely in semiconductors. In the early days, excitons were viewed as hydrogen-like excitations in semiconductors, manifesting as sharp optical absorption peaks superimposed on the broader onset of electron–hole continuum excitations [2, 3]. These optically excited excitons have finite lifetime and eventually decay. When the electromagnetic field is quantized and its full dynamics is included, photons can hybridize with excitons to form mixed light–matter quasiparticles known as exciton-polaritons [4]. By continuously pumping photons to maintain a non-equilibrium steady state, one can realize long-lived exciton-polaritons and even make them condensate [5].

Can excitons and their condensates be stabilized in equilibrium? Inspired by the BCS theory of superconductivity [6], theorists proposed an affirmative answer in the 1960s [7–9]. A BCS-like ground state of excitons is known as the excitonic insulator [9]. The essential condition for the spontaneous formation of excitons is that their binding energy exceeds the band gap [10, 11]. However, excitons are charge-neutral and therefore insensitive to conventional charge transport measurements. With the advent of advanced fabrication techniques for two-dimensional materials at the end of the 20th century, it became possible to engineer spatially separated electron–hole bilayers. This realization opened the door to interlayer excitons, where the electron and hole reside in different layers [12–16]. Numerous efforts have since been made to create exciton condensates in such bilayer systems, with early experiments in the quantum Hall regime providing suggestive evidence for such a phase [17]. More recently, equilibrium exciton fluid has also been realized in layered 2D materials without magnetic fields [18–22]. A major advantage of electron–hole bilayer systems is the ability to probe excitonic states through transport techniques, particularly by Coulomb drag experiments [23].

In the exciton condensate phase, one expects a dissipationless, perfect Coulomb drag, where a current in one layer induces an equal and opposite current in the other layer—a hallmark of the formation of tightly bound, interlayer excitons [20, 24, 25].

However, perfect Coulomb drag alone is insufficient to identify a dissipationless exciton superfluid phase [25]. An important challenge in exciton physics is therefore to unambiguously distinguish between an excitonic insulator, in which electron–hole pairs form without global coherence, and an exciton superfluid, where macroscopic phase coherence enables dissipationless counterflow. This requires transport signatures that directly probe phase stiffness rather than mere pairing. In this Letter, we show that a spin–orbit–coupled bilayer system can host a finite-momentum exciton condensate exhibiting a perfect nonreciprocal Coulomb drag—which we call *coherent-exciton diode effect* (CEDE). This nonreciprocal drag requires global phase-coherent superflow, providing a smoking-gun signature of exciton superfluidity.

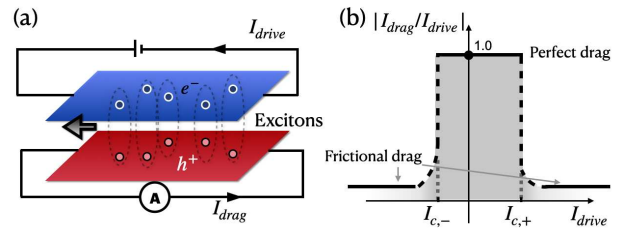


**FIG. 1:** (a) An illustration of Coulomb drag experiment. A current  $I_{\text{drive}}$  in top layer will spontaneously induce  $I_{\text{drag}}$  in bottom layer. (b) A schematic plot for drag ratio  $\zeta = |I_{\text{drag}}/I_{\text{drive}}|$ : at small  $I_{\text{drive}}$ ,  $|\zeta|$  is close to 1, corresponding to the perfect Coulomb drag; as  $I_{\text{drive}}$  exceeds its critical value  $I_{c,\pm}$  in either direction, the condensate is broken down, corresponding to the transition to the frictional drag regime between the two Fermi liquids on each layer [23].

Our work is inspired by previous seminal studies on supercurrent diode effects in superconductors [26–31]. In recent years, it has been shown that breaking parity ( $\mathcal{P}$ ) and time-reversal ( $\mathcal{T}$ ) symmetries in superconductors can not only induce unconventional condensates—such as helical superconductors [32], Fulde–Ferrell–Larkin–Ovchinnikov (FFLO) states [33, 34], and p-wave spin-triplet superconductors [35]—but also lead to nonreciprocity of the superconducting critical current, known as the supercurrent diode effect. This phenomenon has been observed in both bulk superconductors [26, 36, 37] and Josephson junctions [38–41].

We propose that CEDE can arise in asymmetric spin–orbit coupled electron–hole bilayer systems. Experimentally, this may be realized in a sandwich structure, where the top and bottom layers—e.g. transition-metal dichalcogenide materials—have distinct spin–orbit coupling [42]. FIG. 1.(a) shows schematics of the proposed setup. An electric current  $I_{\text{drive}}$  which flows through the top layer can induce a spontaneous drag current  $I_{\text{drag}}$  in the bottom layer, characterized by the dimensionless drag ratio

$$\zeta = \frac{I_{\text{drag}}}{I_{\text{drive}}}. \quad (1)$$

In the weakly correlated regime, perturbation theory yields the so-called frictional drag with  $\zeta \ll 1$  [23]. In contrast, when interlayer exciton forms, the drag becomes nearly perfect, approaching  $\zeta = -1$ . Previous studies have discussed nonreciprocal frictional drag effects arising from broken spatial inversion  $\mathcal{P}$  and time-reversal  $\mathcal{T}$  symmetries, as well as the possibility of nonreciprocal frictional drag [43, 44]. However, the nonreciprocal properties of perfect Coulomb drag remain unexplored. As illustrated in FIG. 1.(b), nonreciprocal perfect Coulomb drag manifests as a plateau with  $|\zeta| = 1$ , bounded by direction-dependent critical currents  $I_{c-}$  and  $I_{c+}$ . When these critical currents differ  $I_{c-} \neq I_{c+}$  the plateau becomes directionally biased, marking the onset of the coherent-exciton diode effect.

*The model.*— We consider a bilayer system composed of two-dimensional semiconductors whose conduction and valence bands have different SOC strengths. By electrostatic gating, the top layer is electron-doped into its conduction band, while the bottom layer is hole-doped into its valence band. The low-energy bands closest to the Fermi level in both layers, together with their corresponding dispersions, are illustrated in FIG. 2.(a). To access the spin degree of freedom, we include both an out-of-plane Zeeman field  $J$  and in-plane Zeeman field  $B$ . Combined with the Rashba SOC strengths  $\lambda_{e,h}$  in the top/bottom layer, the resulting effective noninteracting Hamiltonian at each layer can be written as:

$$H_a = \left( \frac{k^2}{2m_a} - \mu_a \right) + \lambda_a (k_x \sigma_y - k_y \sigma_x) + B \sigma_y + J \sigma_z \quad (2)$$

Here,  $a = e, h$  represents top electron-doped layer and bottom hole-doped layer respectively. We consider the case where  $m_e = m_h$ , and  $\lambda_e > \lambda_h = 0$  [45]. The out-of-plane Zeeman term splits the electron bands and hole bands, and one can assume low-energy carriers are spin polarized in the opposite direction. The dispersion relations at each layer are (We adopt natural units with  $\hbar = c = 1$  throughout the paper and restore them when needed.)

$$\xi_{a,k} = \frac{k^2}{2m_a} - \mu_a - |\lambda_a| \sqrt{\left( k_x + \frac{B}{\lambda_a} \right)^2 + k_y^2 + \left( \frac{J}{\lambda_a} \right)^2} \quad (3)$$

Because of the non-vanishing  $\lambda_e$  and  $B$  terms in the electron dispersion, both inversion ( $\mathcal{P}$ ) and time-reversal ( $\mathcal{T}$ ) symmetries are broken. Consequently, the electron band acquires a non-parabolic form, and its Fermi contour becomes non-circular, as illustrated in FIG. 2.(b). In comparison with the red circular Fermi contour of holes in the bottom layer, the electron Fermi contour exhibits a simultaneous shift and distortion, which together energetically favor an exciton with a finite center-of-mass momentum,  $\mathbf{q}$  (orange arrow in FIG. 2.(b)), which is determined variationally through energy minimization (see later).

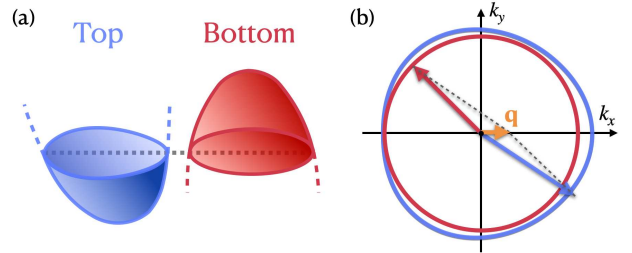


**FIG. 2:** (a) Electron dispersions and Fermi energies in both layers. Gating, spin–orbit coupling, and Zeeman fields create an electron Fermi sea in the top layer and a hole Fermi sea in the bottom layer. The gray dashed line marks the Fermi energy. (b) Schematic of electron and hole Fermi contours. The distortion and shift of the electron contour indicate finite-momentum  $\mathbf{q}$  electron–hole pairing .

Interlayer Coulomb attraction between electrons in top layer and holes in bottom layer is essential for the formation of the exciton. The screened interlayer Coulomb interaction is  $V(x, y) = -e^2/\epsilon\sqrt{x^2 + y^2 + d^2}$ , where  $\epsilon$  is taken as the dielectric constant of the intermediate insulating layer [46],  $d$  is the distance between the layers in  $z$  direction. The second quantized interaction Hamiltonian reads:

$$V_{eh} = -\frac{1}{V} \sum_{k_1, k_2, p} V(p) \psi_{\mathbf{k}_1 + \mathbf{p}}^\dagger \chi_{\mathbf{k}_2 - \mathbf{p}}^\dagger \chi_{\mathbf{k}_2} \psi_{\mathbf{k}_1} \quad (4)$$

where  $V(p) = [2\pi e^2/\epsilon|\mathbf{p}|]e^{-|\mathbf{p}|d}$ ,  $V$  is volume of the sample. We could rewrite the interaction Hamiltonian in an

expansion form of spherical harmonics [47], i.e.,

$$V_{eh} = -\frac{1}{\mathcal{V}} \sum_{k,k',q} V(k-k') \psi_{k+q/2}^\dagger \chi_{-k+q/2}^\dagger \chi_{-k'+q/2} \psi_{k'+q/2}$$

where  $V(k-k') = \sum_{l=0}^{\infty} \sum_{m=-l}^l V_l(|\mathbf{k}|, |\mathbf{k}'|) Y_l^m(\hat{\mathbf{k}}) Y_l^{m*}(\hat{\mathbf{k}}')$ . In the spirit of the pairing approximation [48], we keep the single center-of-mass momentum  $\mathbf{q}$  and  $l=0$  i.e.  $s$ -wave terms only [12, 14, 49]. With this, the effective interaction Hamiltonian is simplified to

$$V_{pair} = -\frac{g}{\mathcal{V}} \sum_{k,k'} \psi_{\mathbf{k}+\mathbf{q}/2}^\dagger h_{-\mathbf{k}+\mathbf{q}/2}^\dagger h_{-\mathbf{k}'+\mathbf{q}/2} \psi_{\mathbf{k}'+\mathbf{q}/2} \quad (5)$$

where  $g \approx \frac{\pi(1-e^{-2k_F d})}{ek_F^2 d^2} e^2$  is the effective s-wave interaction strength, which is suppressed when increasing  $d$ , and  $k_F = (4\pi)^{-1} \sum_{a=e,h} \int d\phi \sqrt{\mathbf{k}^2} (\xi_{a,k} = 0)$  is the (average) Fermi momentum.  $\phi$  is the azimuthal angle of  $\mathbf{k}$  so that  $\mathbf{k} = (|\mathbf{k}| \cos \phi, |\mathbf{k}| \sin \phi)$ .

*Ginzburg-Landau theory and finite momentum condensate.*— Based on the above, the second-quantized effective Hamiltonian is  $H = H_0 + V_{pair}$ , where

$$H_0 = \sum_k \xi_{e,k} \psi_k^\dagger \psi_k + \xi_{h,k} \chi_k^\dagger \chi_k \quad (6)$$

and  $V_{pair}$  is given in (5). We take the Fulde-Ferrell-type [33] ansatz solution for the excitonic order parameter field  $\Delta(\mathbf{x}) = \Delta e^{i\mathbf{q} \cdot \mathbf{x}}$ , where  $\mathbf{q}$  is the exciton momentum. Performing a Hubbard-Stratonovich transformation yields the effective Euclidean action  $S[\bar{\Delta}, \Delta]$ :

$$e^{-S[\bar{\Delta}, \Delta]} = e^{-\int_0^\beta d\tau \frac{\mathcal{V}}{g} (\bar{\Delta} \Delta)} \int D(\bar{\psi}, \psi) D(\bar{\chi}, \chi) e^{-S_{BdG}} \quad (7)$$

where  $S_{BdG} = \int d\tau \sum_k [\bar{\psi}_k (\partial_\tau + \xi_{e,k}) \psi_k + \bar{\chi}_k (\partial_\tau + \xi_{h,k}) \chi_k - (\bar{\Delta} \chi_{-k+q/2} \psi_{k+q/2} + h.c.)]$ . Near the phase transition point (i.e.,  $\Delta \ll k_B T_c$ ), we keep the leading terms in  $S[\bar{\Delta}, \Delta] = T^{-1} F[\bar{\Delta}, \Delta]$ , and derive Ginzburg-Landau Free energy

$$F[\bar{\Delta}, \Delta] = \alpha(T, \mathbf{q}) |\Delta|^2 + \frac{1}{2} \beta(T, \mathbf{q}) |\Delta|^4 + O(|\Delta|^6) \quad (8)$$

where

$$\begin{aligned} \alpha(T, \mathbf{q}) &= \frac{\mathcal{V}}{g} + \sum_{n,k} \frac{T}{(-i\omega_n + \xi_{e,\mathbf{k}+\frac{\mathbf{q}}{2}})(-i\omega_n - \xi_{h,-\mathbf{k}+\frac{\mathbf{q}}{2}})} \\ \beta(T, \mathbf{q}) &= \sum_{n,k} \frac{T}{(-i\omega_n + \xi_{e,\mathbf{k}+\frac{\mathbf{q}}{2}})^2 (-i\omega_n - \xi_{h,-\mathbf{k}+\frac{\mathbf{q}}{2}})^2} \end{aligned} \quad (9)$$

and  $\omega_n = (2n+1)\pi T$  with  $n = 0, \pm 1, \pm 2, \dots$  are the fermionic Matsubara frequencies. It is evident from (9) that, if  $\xi_{e,\mathbf{k}} = \xi_{e,-\mathbf{k}}$  and  $\xi_{h,\mathbf{k}} = \xi_{h,-\mathbf{k}}$ , both  $\alpha$  and  $\beta$  are even functions of  $\mathbf{q}$ , and therefore no odd-exponent terms appear in the small- $\mathbf{q}$  expansion. As previously pointed out, the presence of terms odd in  $\mathbf{q}$  is essential

for realizing finite-momentum condensates and supercurrent diode effect [27–29]. Therefore, our model requires  $\xi_{e,\mathbf{k}} \neq \xi_{e,-\mathbf{k}}$ , which occurs when both inversion and time-reversal symmetries are broken induced by a nonzero in-plane Zeeman field  $B$ .

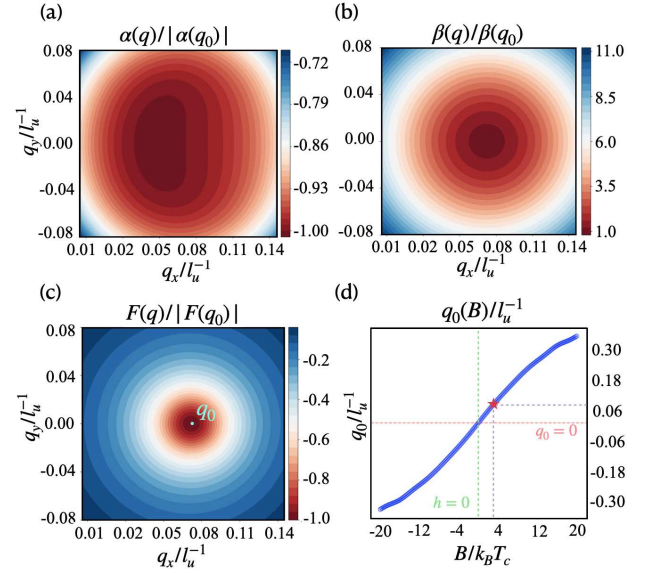


**FIG. 3:** (a) Exciton condensate momentum  $q_0$  as a function of  $B/k_B T_c$  at  $0.90 T_c$ . At  $B/k_B T_c=3.0$ , we calculate the Ginzburg-Landau coefficients of the condensate as a function of exciton momentum  $(q_x, q_y)$ , based on which we calculate free energy and extract  $q_0$ . (b, c, d) Normalized values of  $\alpha(\mathbf{q})$ ,  $\beta(\mathbf{q})$  and  $F(\mathbf{q})$  at  $T/T_c = 0.90$ ,  $B/k_B T_c = 3.0$ , where red dot represents exciton momentum  $\mathbf{q}_0$  that minimizes  $F(\mathbf{q})$ .  $E_u = k_B T_c$  and  $l_u = \hbar/\sqrt{m_e k_B T_c}$  are energy and length units, respectively.

In the Ginzburg-Landau framework, physical quantities of interest can be expressed in terms of  $\alpha$  and  $\beta$ . For instance, free energy  $F(\mathbf{q}) = -[\alpha(\mathbf{q})]^2/\beta(\mathbf{q})$ , and the supercurrent density  $J_i(\mathbf{q}) = (\hbar\mathcal{V})^{-1} \partial F(\mathbf{q})/\partial q_i$ . Based on expressions (9), we numerically calculated the  $q_x$  and  $q_y$ -dependence of  $\alpha(T, \mathbf{q})$  and  $\beta(T, \mathbf{q})$  at  $T/T_c = 0.90$ ,  $B/k_B T_c = 3.0$  (FIG. 3.(a, b)). Within the exciton momentum range shown in the figure,  $\alpha < 0$  and  $\beta > 0$ , ensures condensation. For exciton momenta away from the center of the figure, excitons flow, and the order parameter  $\Delta = |\alpha|/\beta$  is suppressed as expected. Furthermore, we plot the  $q_x, q_y$ -dependence of the free energy  $F$  in FIG. 3.(c). Treating  $\mathbf{q} = (q_x, q_y)$  as a variational parameter, the exciton condensate at the momentum  $\mathbf{q}_0 = (q_0, 0)$  at which the free energy is minimized. We show the  $B$ -dependence of the optimal  $q_0$  in FIG. 3.(d), showing a monotonically increase with the in-plane Zeeman field  $B$ .

*Coherent Exciton diode effect.*— The excitonic supercurrent density as a function of exciton momentum  $\mathbf{q}$  is  $J_i(\mathbf{q}) = (\hbar\mathcal{V})^{-1} \partial F(\mathbf{q})/\partial q_i$ , which vanishes in ground state at  $\mathbf{q} = \mathbf{q}_0$ . At  $0.9 T_c$ , we focus on the  $x$ -direction,

where the mirror symmetry is broken, and plot the numerical values  $J_x(q_x, q_y)$  at  $B/k_B T_c = 3.0$  in FIG. 4.(a). As  $q_x$  is varied to generate a nonzero supercurrent  $J_x$ , we obtain a minimum  $J_{c-}$  and a maximum  $J_{c+}$ , which we identify as critical currents in two opposite directions along the  $x$  axis [50–52]. In the presence of either  $\mathcal{P}$  or  $\mathcal{T}$  symmetry, the relation  $|J_{c+}| = |J_{c-}|$  must hold. However, when both symmetries are broken—as in our model—this constraint no longer applies, and we indeed find  $J_{c+} \neq J_{c-}$ . Each exciton possesses an electric dipole oriented along the  $-z$  direction, so the excitonic diode effect in the bilayer may be naturally viewed as a supercurrent diode effect of electric dipoles [53, 54].

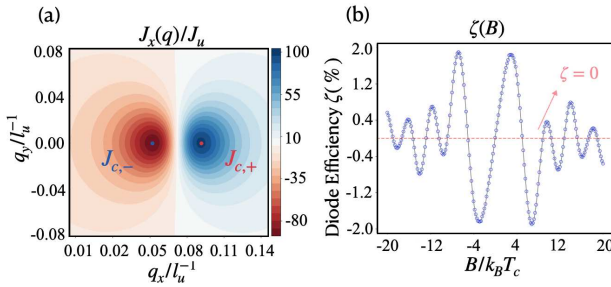


**FIG. 4:** (a) Supercurrent density  $J_x$  as a function of exciton momentum  $q_x$  at  $T/T_c = 0.90, B/k_B T_c = 3.0$ . (b) At  $T/T_c = 0.90$ , diode efficiency  $\eta$  as a function of  $B/k_B T_c$ .

In FIG. 4.(a), we extract  $J_{c+}/J_u = 98.4$ ,  $J_{c-}/J_u = -94.8$ . Using typical model parameters, we estimate  $|J_{c+}| - |J_{c-}|$  to be on the order of  $10 \text{ } (\mu\text{A})(\mu\text{m})^{-1}$ , which is well within experimental reach. The diode efficiency, defined as  $\eta = (|J_{c+}| - |J_{c-}|) / (|J_{c+}| + |J_{c-}|)$ , is shown as a function of the external in-plane field  $h$  in FIG. 4.(b). Interestingly,  $\eta$  does not increase monotonically with  $h$  but instead exhibits irregular oscillations. At certain values of  $h$ ,  $\eta$  even vanishes, showing the absence of a supercurrent diode effect. This behavior demonstrates that, while breaking both  $\mathcal{P}$  and  $\mathcal{T}$  symmetries is necessary for the emergence of a supercurrent diode effect, it is not sufficient. Our numeric simulations reveal a nonlinear oscillatory behavior in the diode efficiency, displaying quasiperiodicity over scales of several  $k_B T_c$ . This nonlinear behavior stems from our investigation of the condensate's breakdown current [55].

*Frictional Coulomb drag in the normal phase.*— When the excitonic supercurrent exceeds the critical current, the drag ratio doesn't drop to 0 but remains a finite small value, as shown in FIG. 1.(b). Such remaining drag effect away from the condensate phase is called frictional Coulomb drag [23]. This originates from momentum transfer between the charge carriers in different layers, which has been studied in a series delicate works using kinetic theory [23, 56, 57]. Flowing charge carriers in the drive layer (layer 1) will exert a force on carriers in the drag layer (layer 2), which in the steady state has to be balanced out by either electrical force or frictional

force.

In our system, the top layer contains electrons with a dispersion that breaks both  $\mathcal{P}$  and  $\mathcal{T}$  symmetries, while the bottom layer consists of holes with parabolic dispersion, as shown in (3). We calculate the drag ratio in the  $x$ -direction. To the linear order, the current in the top layer  $j_1$  and bottom layer  $j_2$  satisfied  $j_2 = \zeta \cdot j_1$ , where the expression for  $\zeta$  is derived in the Supplemental Materials [55]

$$\zeta = -\frac{n_h \bar{m}_{e,x}}{n_e m_h} \cdot \frac{1}{(\tau_D^I/\tau_D^{II}) + (\tau_D^I/\tau_2)} \quad (10)$$

where  $n_{e,h}$  are charge carrier densities in either layer.  $\bar{m}_{e,x}^{-1} = n_e^{-1} \int \frac{d^2 k}{(2\pi)^2} f_0(\xi_{e,k}) \partial_{k_x}^2 \xi_{e,k}$  is the ensemble average of inverse effective mass in  $x$  direction with  $f_0(\xi) = (e^{\beta\xi} + 1)^{-1}$  the Fermi-Dirac distribution function. The scattering time  $\tau_D^{I,II}$  are provided in Supplemental materials [55]. For our parameters, a rough estimate yields  $\tau_D^I \approx \tau_D^{II} \approx 1 \times 10^{-7} \text{ s}$ , assuming the Fermi energies are  $E_{Fe} \approx E_{Fh} \approx 10 \text{ meV}$  at  $T = 10 \text{ K}$ . In a clean sample, one often takes  $\tau_2 \approx 1-2 \times 10^{-9} \text{ s}$ , leading to a drag ratio of  $\zeta \approx 1\%$ . As the Fermi energies decrease, both  $\tau_D^{-1}$  and  $\zeta$  increase, consistent with Ref. [56]. It is important to note that this analysis can be extended to higher-order processes, where simultaneous breaking of  $\mathcal{P}$  and  $\mathcal{T}$  symmetries may lead to a nonlinear, nonreciprocal drag effect [58, 59]. While these higher-order effects are beyond the main focus of this work, a brief discussion is provided in the Supplemental Materials [55].

*Conclusion & Outlook.*— We proposed the coherent-exciton diode effect, which gives a robust signature of interlayer exciton condensation through a nonreciprocal Coulomb drag response. Using typical experimental parameters, i.e., critical temperature  $T_c = 10 \text{ K}$  and effective electron mass of  $m_e \approx 0.2 m_0$  ( $m_0$  is the bare electron mass), the characteristic exciton condensate momentum is estimated as  $q_0 = 0.2 l_u^{-1} \approx 0.2 \sqrt{m_e k_B T_c / \hbar^2}$ , corresponding to a phase modulation wavelength of  $\lambda \approx 600 \text{ nm}$ —well within current experimental reach. For a sample with a width of  $1 \mu\text{m}$ , the critical current can reach  $I_c \approx 1 \text{ mA}$ , resulting in an expected current difference of  $\delta I \approx 10 \mu\text{A}$  given a diode efficiency of  $\eta = 1\%$ . Such signals should be readily detectable in two-dimensional layered materials with strong spin-orbit coupling, such as transition-metal dichalcogenides (TMD) [60]. In particular, to realize Rashba spin-orbit coupling instead of Ising spin-orbit coupling, one can use Janus TMD, which breaks inversion symmetry in  $z$ -direction intrinsically [61, 62].

The electron-hole bilayer system, with its remarkable tunability, provides an ideal platform for realizing a broad spectrum of exotic quantum states. For instance, excitons have been observed in both the weak-coupling BCS limit and the strong-coupling BEC limit [63], unlocking new possibilities for exploring the BCS-BEC

crossover in solid-state systems [64]. An in-plane electric field can dissociate exciton pairs, inducing a many-body breakdown mechanism [46], and several other experimental signatures have also been proposed and detected [65–68]. Moreover, gating imbalance in electron–hole bilayers could lead to a wealth of intriguing physics, such as excitonic FFLO states [69–71], or time-reversal broken topologically ordered ground states [72]. When electron–hole densities are imbalanced yet commensurate, the system favors the formation of exotic three-body bound states, such as trions [73–77]. In this rich landscape of physics, our proposed coherent-exciton diode effect opens a novel and intriguing avenue for detecting and manipulating exotic excitonic states, offering a promising route to realize new quantum devices based on excitonic transport and nonreciprocal behaviors.

*Acknowledgment.*— The authors are grateful to Gabriel Cardoso for useful discussions throughout the project and detailed suggestions to the manuscript. The authors acknowledge Thors Hans Hansson for insightful discussions and constructive suggestions. J.X. Hui thanks Xiaodong He and Xiaotong Chen for their generous help with numerical calculations. The authors also appreciate James Jun He, Noah F.Q. Yuan, Xiaoxue Liu and Shengwei Jiang for useful discussions. This work was supported by National Natural Science Foundation of China (NSFC) under Grant No. 12374332, the Innovation Program for Quantum Science and Technology Grant No. 2021ZD0301900, Cultivation Project of Shanghai Research Center for Quantum Sciences Grant No. LZPY2024, and Shanghai Science and Technology Innovation Action Plan Grant No. 24LZ1400800.

- [10] V. M. Pereira, Topological excitons, *Nature Physics* **18**, 6 (2022).
- [11] M. Xie and A. H. MacDonald, Electrical reservoirs for bilayer excitons, *Physical review letters* **121**, 067702 (2018).
- [12] Y. E. Lozovik and V. Yudson, A new mechanism for superconductivity: pairing between spatially separated electrons and holes, *Zh. Eksp. Teor. Fiz.* **71**, 738 (1976).
- [13] M. Fogler, L. Butov, and K. Novoselov, High-temperature superfluidity with indirect excitons in van der waals heterostructures, *Nature communications* **5**, 4555 (2014).
- [14] D. Fil and S. Shevchenko, Electron-hole superconductivity, *Low Temperature Physics* **44**, 867 (2018).
- [15] J. Zhu and S. Das Sarma, Interaction and coherence in two-dimensional bilayers, *Physical Review B* **109**, 085129 (2024).
- [16] H. Yang, X. Dai, and X.-Z. Li, Exciton insulators in two-dimensional systems, *Chinese Physics B* (2025).
- [17] J. Eisenstein, Exciton condensation in bilayer quantum hall systems, *Annu. Rev. Condens. Matter Phys.* **5**, 159 (2014).
- [18] Z. Wang, D. A. Rhodes, K. Watanabe, T. Taniguchi, J. C. Hone, J. Shan, and K. F. Mak, Evidence of high-temperature exciton condensation in two-dimensional atomic double layers, *Nature* **574**, 76 (2019).
- [19] L. Ma, P. X. Nguyen, Z. Wang, Y. Zeng, K. Watanabe, T. Taniguchi, A. H. MacDonald, K. F. Mak, and J. Shan, Strongly correlated excitonic insulator in atomic double layers, *Nature* **598**, 585 (2021).
- [20] P. X. Nguyen, L. Ma, R. Chaturvedi, K. Watanabe, T. Taniguchi, J. Shan, and K. F. Mak, Perfect coulomb drag in a dipolar excitonic insulator, *Science* **388**, 274 (2025).
- [21] P. X. Nguyen, R. Chaturvedi, B. Zou, K. Watanabe, T. Taniguchi, A. H. MacDonald, K. F. Mak, and J. Shan, Quantum oscillations in a dipolar excitonic insulator, *Nature Materials* **1** (2025).
- [22] B. H. Moon, A. Mondal, D. K. Efimkin, and Y. H. Lee, Exciton condensate in van der waals layered materials, *Nature Reviews Physics* **1** (2025).
- [23] B. Narozhny and A. Levchenko, Coulomb drag, *Reviews of Modern Physics* **88**, 025003 (2016).
- [24] D. Nandi, A. Finck, J. Eisenstein, L. Pfeiffer, and K. West, Exciton condensation and perfect coulomb drag, *Nature* **488**, 481 (2012).
- [25] R. Qi, A. Y. Joe, Z. Zhang, J. Xie, Q. Feng, Z. Lu, Z. Wang, T. Taniguchi, K. Watanabe, S. Tongay, *et al.*, Perfect coulomb drag and exciton transport in an excitonic insulator, *Science* **388**, 278 (2025).
- [26] F. Ando, Y. Miyasaka, T. Li, J. Ishizuka, T. Arakawa, Y. Shiota, T. Moriyama, Y. Yanase, and T. Ono, Observation of superconducting diode effect, *Nature* **584**, 373 (2020).
- [27] N. F. Yuan and L. Fu, Supercurrent diode effect and finite-momentum superconductors, *Proceedings of the National Academy of Sciences* **119**, e2119548119 (2022).
- [28] J. J. He, Y. Tanaka, and N. Nagaosa, A phenomenological theory of superconductor diodes, *New Journal of Physics* **24**, 053014 (2022).
- [29] A. Daido, Y. Ikeda, and Y. Yanase, Intrinsic superconducting diode effect, *Physical Review Letters* **128**, 037001 (2022).
- [30] M. Nadeem, M. S. Fuhrer, and X. Wang, The super-

\* qingdong.jiang@sjtu.edu.cn

- [1] J. Frenkel, On the transformation of light into heat in solids. i, *Physical Review* **37**, 17 (1931).
- [2] M. Sturge, Optical absorption of gallium arsenide between 0.6 and 2.75 ev, *Physical Review* **127**, 768 (1962).
- [3] O. Karni, E. Barré, V. Pareek, J. D. Georgaras, M. K. Man, C. Sahoo, D. R. Bacon, X. Zhu, H. B. Ribeiro, A. L. O’Beirne, *et al.*, Structure of the moiré exciton captured by imaging its electron and hole, *Nature* **603**, 247 (2022).
- [4] J. Hopfield, Theory of the contribution of excitons to the complex dielectric constant of crystals, *Physical Review* **112**, 1555 (1958).
- [5] D. Snoke, Spontaneous bose coherence of excitons and polaritons, *Science* **298**, 1368 (2002).
- [6] J. Bardeen, L. N. Cooper, and J. R. Schrieffer, Theory of superconductivity, *Physical review* **108**, 1175 (1957).
- [7] J. M. Blatt, K. Böer, and W. Brandt, Bose-einstein condensation of excitons, *Physical Review* **126**, 1691 (1962).
- [8] L. Keldysh and Y. V. Kopaev, Possible instability of the semimetallic state toward coulomb interaction, *Fiz. Tverd. Tela* **6**, 2791 (1964).
- [9] D. Jerome, T. Rice, and W. Kohn, Excitonic insulator, *Physical Review* **158**, 462 (1967).

conducting diode effect, *Nature Reviews Physics* **5**, 558 (2023).

[31] K. Jiang and J. Hu, Superconducting diode effects, *Nature Physics* **18**, 1145 (2022).

[32] V. Mineev and K. Samokhin, Helical phases in superconductors, *Zh. Eksp. Teor. Fiz.* **105**, 747 (1994).

[33] P. Fulde and R. A. Ferrell, Superconductivity in a strong spin-exchange field, *Physical Review* **135**, A550 (1964).

[34] A. Larkin and Y. N. Ovchinnikov, *Zh. è ksp. teor. fiz.* **47**, 1136 1964 sov. phys. *JETP* **20**, 762 (1965).

[35] G. E. Volovik, *The universe in a helium droplet*, Vol. 117 (OUP Oxford, 2003).

[36] T. Le, Z. Pan, Z. Xu, J. Liu, J. Wang, Z. Lou, X. Yang, Z. Wang, Y. Yao, C. Wu, *et al.*, Superconducting diode effect and interference patterns in kagome csv3sb5, *Nature* **630**, 64 (2024).

[37] J.-X. Lin, P. Siriviboon, H. D. Scammell, S. Liu, D. Rhodes, K. Watanabe, T. Taniguchi, J. Hone, M. S. Scheurer, and J. Li, Zero-field superconducting diode effect in small-twist-angle trilayer graphene, *Nature Physics* **18**, 1221 (2022).

[38] H. Wu, Y. Wang, Y. Xu, P. K. Sivakumar, C. Pasco, U. Filippozzi, S. S. Parkin, Y.-J. Zeng, T. McQueen, and M. N. Ali, The field-free josephson diode in a van der waals heterostructure, *Nature* **604**, 653 (2022).

[39] M. Trahms, L. Melischeck, J. F. Steiner, B. Mahendru, I. Tamir, N. Bogdanoff, O. Peters, G. Reecht, C. B. Winkelmann, F. von Oppen, *et al.*, Diode effect in josephson junctions with a single magnetic atom, *Nature* **615**, 628 (2023).

[40] Y. Zhang, Y. Gu, P. Li, J. Hu, and K. Jiang, General theory of josephson diodes, *Physical Review X* **12**, 041013 (2022).

[41] J.-X. Hu, Z.-T. Sun, Y.-M. Xie, and K. Law, Josephson diode effect induced by valley polarization in twisted bilayer graphene, *Physical review letters* **130**, 266003 (2023).

[42] D. Maruyama, M. Sigrist, and Y. Yanase, Locally non-centrosymmetric superconductivity in multilayer systems, *Journal of the Physical Society of Japan* **81**, 034702 (2012).

[43] Y. Fu, Y. Huang, and Q. L. He, Non-reciprocal coulomb drag between chern insulators, *Nature Communications* **16**, 3058 (2025).

[44] D. Zverevich and A. Levchenko, Nonreciprocal coulomb drag in electron bilayers, *arXiv preprint arXiv:2504.08679* (2025).

[45] Note when  $\lambda_e = -\lambda_h$  and  $\mu_e = \mu_h$ , electron Fermi circle and hole Fermi circle are mirror image to each other. Under such condition, both finite-momentum pairing and supercurrent diode effect vanish.

[46] Y. Shao and X. Dai, Electrical breakdown of excitonic insulators, *Physical Review X* **14**, 021047 (2024).

[47] A. J. Leggett, *Quantum liquids: Bose condensation and Cooper pairing in condensed-matter systems* (Oxford university press, 2006).

[48] J. R. Schrieffer, *Theory of superconductivity* (CRC press, 2018).

[49] S. Shevchenko, Theory of superconductivity of systems with pairing of spatially separated electrons and holes, *Soviet Journal of Low Temperature Physics* **2**, 251 (1976).

[50] J. Bardeen, Critical fields and currents in superconductors, *Reviews of modern physics* **34**, 667 (1962).

[51] M. Tinkham, *Introduction to superconductivity* (Courier Corporation, 2004).

[52] P.-G. De Gennes, *Superconductivity of metals and alloys* (CRC press, 2018).

[53] Q.-D. Jiang, Z.-q. Bao, Q.-F. Sun, and X. Xie, Theory for electric dipole superconductivity with an application for bilayer excitons, *Scientific reports* **5**, 11925 (2015).

[54] Y. Shao, H. Shi, and X. Dai, Electromagnetic responses of bilayer excitonic insulators: from exciton london equations to dipole and inverse dipole hall effects, *arXiv preprint arXiv:2509.02142* (2025).

[55] J.-X. Hui and Q.-D. Jiang, Supplemental material for "nonreciprocal perfect coulomb drag in electron-hole bilayers: Coherent exciton superflow as a diode" (2025).

[56] A.-P. Jauho and H. Smith, Coulomb drag between parallel two-dimensional electron systems, *Physical Review B* **47**, 4420 (1993).

[57] A. G. Rojo, Electron-drag effects in coupled electron systems, *Journal of Physics: Condensed Matter* **11**, R31 (1999).

[58] G. Rikken, J. Fölling, and P. Wyder, Electrical magneto-chiral anisotropy, *Physical review letters* **87**, 236602 (2001).

[59] T. Ideue, K. Hamamoto, S. Koshikawa, M. Ezawa, S. Shimizu, Y. Kaneko, Y. Tokura, N. Nagaosa, and Y. Iwasa, Bulk rectification effect in a polar semiconductor, *Nature Physics* **13**, 578 (2017).

[60] E. C. Regan, D. Wang, E. Y. Paik, Y. Zeng, L. Zhang, J. Zhu, A. H. MacDonald, H. Deng, and F. Wang, Emerging exciton physics in transition metal dichalcogenide heterobilayers, *Nature Reviews Materials* **7**, 778 (2022).

[61] A.-Y. Lu, H. Zhu, J. Xiao, C.-P. Chuu, Y. Han, M.-H. Chiu, C.-C. Cheng, C.-W. Yang, K.-H. Wei, Y. Yang, *et al.*, Janus monolayers of transition metal dichalcogenides, *Nature nanotechnology* **12**, 744 (2017).

[62] X. Tang and L. Kou, 2d janus transition metal dichalcogenides: Properties and applications, *physica status solidi (b)* **259**, 2100562 (2022).

[63] X. Liu, J. Li, K. Watanabe, T. Taniguchi, J. Hone, B. I. Halperin, P. Kim, and C. R. Dean, Crossover between strongly coupled and weakly coupled exciton superfluids, *Science* **375**, 205 (2022).

[64] Q. Chen, J. Stajic, S. Tan, and K. Levin, Bcs–bec crossover: From high temperature superconductors to ultracold superfluids, *Physics Reports* **412**, 1 (2005).

[65] Y. Shao and X. Dai, Quantum oscillations in an excitonic insulating electron-hole bilayer, *Physical Review B* **109**, 155107 (2024).

[66] Z. Han, Y. Xia, K. Watanabe, T. Taniguchi, K. F. Mak, and J. Shan, Quantum oscillations between excitonic and quantum spin hall insulators in moiré wse2, *arXiv preprint arXiv:2509.19287* (2025).

[67] R. Qi, Q. Li, Z. Zhang, J. Nie, B. Zou, Z. Cui, H. Kim, C. Sanborn, S. Chen, J. Xie, *et al.*, Competition between excitonic insulators and quantum hall states in correlated electron-hole bilayers, *Nature Materials* **1** (2025).

[68] Y. Shao, H. Shi, and X. Dai, Electromagnetic responses of bilayer excitonic insulators, *arXiv preprint arXiv:2509.02142* (2025).

[69] J. Varley and D. Lee, Structure of exciton condensates in imbalanced electron-hole bilayers, *Physical Review B* **94**, 174519 (2016).

[70] B. Seradjeh, Topological exciton condensate of imbalanced electrons and holes, *Physical Review*

B—Condensed Matter and Materials Physics **85**, 235146 (2012).

[71] A. Kumar, A. S. Patri, and T. Senthil, Unconventional superconductivity mediated by exciton density wave fluctuations, arXiv preprint arXiv:2410.09148 (2024).

[72] R. Wang, T. A. Sedrakyan, B. Wang, L. Du, and R.-R. Du, Excitonic topological order in imbalanced electron-hole bilayers, *Nature* **619**, 57 (2023).

[73] T. Ouyang and S.-F. Shi, Quantum trions in equilibrium, *Science* **390**, 241 (2025).

[74] R. Qi, Q. Li, Z. Zhang, S. Chen, J. Xie, Y. Ou, Z. Cui, D. D. Dai, A. Y. Joe, T. Taniguchi, *et al.*, Electrically controlled interlayer trion fluid in electron-hole bilayers, *Science* **390**, 299 (2025).

[75] P. X. Nguyen, R. Chaturvedi, L. Ma, P. Knuppel, K. Watanabe, T. Taniguchi, K. F. Mak, and J. Shan, An equilibrium trion liquid in atomic double layers, *Science* **390**, 304 (2025).

[76] D. D. Dai and L. Fu, Strong-coupling phases of trions and excitons in electron-hole bilayers at commensurate densities, *Physical Review Letters* **132**, 196202 (2024).

[77] C. Zerba, C. Kuhlenkamp, A. Imamoğlu, and M. Knap, Realizing topological superconductivity in tunable bose-fermi mixtures with transition metal dichalcogenide heterostructures, *Physical Review Letters* **133**, 056902 (2024).

# Supplemental Materials for “Nonreciprocal Perfect Coulomb Drag in Electron–Hole Bilayers: Coherent Exciton Superflow as a Diode”

Jun-Xiao Hui

*Tsung-Dao Lee Institute, Shanghai Jiao Tong University, Shanghai 200240, China and School of Physics and Astronomy, Shanghai Jiao Tong University, Shanghai 200240, China*

Qing-Dong Jiang\*

*Tsung-Dao Lee Institute, Shanghai Jiao Tong University, Shanghai 200240, China  
School of Physics and Astronomy, Shanghai Jiao Tong University, Shanghai 200240, China and  
Shanghai Branch, Hefei National Laboratory, Shanghai 201315, China*

(Dated: February 4, 2026)

## Supplemental Materials

### S-I. Rashba-Zeeman-Ising Model

We consider the effective Hamiltonian of a two-dimensional direct band gap semiconductor, where the conduction band has considerable Rashba spin-orbit coupling(SOC) with strength  $\lambda$  though the valence band doesn't have. Such a band structure can be realized in Janus TMD material[1, 2] or artificially engineered systems. We apply Zeeman field  $B$  in  $y$  direction and also  $J$  in  $z$  direction, then the conduction band and valence band Hamiltonian are written as:

$$\mathcal{H}_c(k) = \frac{\delta}{2} + \frac{k^2}{2m_e} + \lambda(k_x\sigma_y - k_y\sigma_x) + B\sigma_y + J\sigma_z - \mu \quad (1)$$

$$\mathcal{H}_v(k) = -\frac{\delta}{2} - \frac{k^2}{2m_h} + B\sigma_y + J\sigma_z - \mu \quad (2)$$

respectively.  $\delta$  is the band gap.  $\mu, h$  are the chemical potentials which can be tuned by electrical gating. When  $\mu > \delta/2$ , the system has electron charge carriers and when  $\mu < -\delta/2$  the system has hole as charge carriers. We diagonalize the Hamiltonian in two  $2 \times 2$  spinor spaces and find the dispersions to be:

$$\xi_{c,\pm}(k) = \frac{k^2}{2m_e} \pm \lambda\sqrt{(k_x + B/\lambda)^2 + k_y^2 + (J/\lambda)^2} - (\mu - \frac{\delta}{2}) \quad (3)$$

$$\xi_{v,\pm}(k) = -\frac{k^2}{2m_h} \pm \sqrt{B^2 + J^2} - (\mu + \frac{\delta}{2}) \quad (4)$$

Due to the presence of  $z$ -direction Zeeman field, gaps of order  $\sqrt{J^2 + B^2}$  are opened between two conduction bands and two valence bands, which offers a way to isolate one of them among the four: If we set  $\delta/2 - J < \mu < \delta/2 + J$ , the Fermi surface only cut the  $\xi_{c,-}$  band; If we set  $-\delta/2 - \sqrt{J^2 + B^2} < \mu < -\delta/2 + \sqrt{J^2 + B^2}$ , the Fermi surface only cuts the  $\xi_{v,-}$  band.

Now consider double layer setup as presented in the main text of the paper, we set  $\delta/2 - J < \mu_{top} < \delta/2 + J$  and  $-\delta/2 - \sqrt{J^2 + B^2} < \mu_{bottom} < -\delta/2 + \sqrt{J^2 + B^2}$  and end up with a single-component electron gas in top layer and a single-component hole gas in bottom layer. The two fermion gases attracts each other by Coulomb interaction. At low temperature, they tend to form excitonic bound state and Bose-Einstein condensation.

### S-II. Functional Approach to Bilayer Exciton Condensate

In the model presented in previous Section, we isolate the lower conduction band in the top layer and upper valence band in the bottom layer. Introducing hole creation/annihilation operators  $\chi_k = c_{-k}^\dagger$  in bottom layer, we end up with a two-species fermion system. The effective second-quantized Hamiltonian is:

$$H = \sum_k (\xi_{e,k} \psi_k^\dagger \psi_k + \xi_{h,k} \chi_k^\dagger \chi_k) + V_{eh} \quad (5)$$

Where  $\xi_{e,k} = \frac{k^2}{2m_e} - \lambda\sqrt{(k_x + (B/\lambda))^2 + k_y^2 + (J/\lambda)^2} - E_{Fe}$ ,  $\xi_{h,k} = \frac{k^2}{2m_\mu} - E_{Fh}$ .  $E_{Fe}, E_{Fh}$  measure the energy difference from Fermi level to band bottoms. The form of  $V_{eh}$  is presented in the main text, which can be written as  $-(g/\mathcal{V})\sum_{k,k'}\psi_{k+q/2}^\dagger\chi_{-k+q/2}^\dagger\chi_{-k'+q/2}\psi_{k'+q/2}$  under  $s$ -wave,  $q$ -momentum pairing approximation. In the functional integral formalism, the action reads:

$$S[\psi^\dagger, \psi, \chi^\dagger, \chi] = \int d\tau \sum_k (\psi_k^\dagger(\partial_\tau + \xi_{e,k})\psi_k + \chi_k^\dagger((\partial_\tau + \xi_{h,k}))\chi_k) - \frac{g}{\mathcal{V}} \sum_{k,k'} \psi_{k+q/2}^\dagger \chi_{-k+q/2}^\dagger \chi_{-k'+q/2} \psi_{k'+q/2} \quad (6)$$

We perform the Hubbard-Stratonovich transformation and extract the effective theory of excitonic order parameter field[3, 4]:

$$\mathcal{Z} = \int D(\psi^\dagger, \psi, \chi^\dagger, \chi) \exp\{-S[\psi^\dagger, \psi, \chi^\dagger, \chi]\} \quad (7)$$

$$= \int D(\bar{\Delta}, \Delta) \int D(\psi^\dagger, \psi, \chi^\dagger, \chi) \exp\{-\int d\tau [\frac{\mathcal{V}}{g} \bar{\Delta} \Delta + \sum_k (\psi_k^\dagger(\partial_\tau + \xi_{e,k})\psi_k + \chi_k^\dagger((\partial_\tau + \xi_{h,k}))\chi_k) \quad (8)$$

$$- \bar{\Delta} \chi_{-k+q/2} \psi_{k+q/2} - \psi_{k+q/2}^\dagger \chi_{-k+q/2}^\dagger \Delta)]\} \quad (9)$$

$$= \int D(\bar{\Delta}, \Delta) \exp\{-\Gamma[\bar{\Delta}, \Delta]\} \quad (10)$$

Where

$$\exp\{-\Gamma[\bar{\Delta}, \Delta]\} = \exp\{-\int d\tau \frac{\mathcal{V}}{g} \bar{\Delta} \Delta\} \int D(\psi^\dagger, \psi, \chi^\dagger, \chi) \exp\{-\int d\tau \sum_k (\psi_{k+q/2}^\dagger \chi_{-k+q/2}) \quad (11)$$

$$\times \begin{pmatrix} \partial_\tau + \xi_{e,k+q/2} & -\Delta \\ -\bar{\Delta} & \partial_\tau - \xi_{h,-k+q/2} \end{pmatrix} \begin{pmatrix} \psi_{k+q/2} \\ \chi_{-k+q/2}^\dagger \end{pmatrix}\} \quad (12)$$

$$= \exp\{-\frac{\mathcal{V}\beta}{g} \bar{\Delta} \Delta + \sum_{n,k} \ln[(-i\omega_n + \xi_{e,k+q/2})(-i\omega_n - \xi_{h,-k+q/2}) - \bar{\Delta} \Delta]\} \quad (13)$$

$$= \exp\{-\beta F[\bar{\Delta}, \Delta]\} \quad (14)$$

Where we have neglected temporal fluctuation by assuming  $\Delta(\tau) \equiv \Delta$ , which can be justified near transition temperature[5]. The free energy functional is defined as

$$F[\bar{\Delta}, \Delta] = T\Gamma[\bar{\Delta}, \Delta] \quad (15)$$

$$= \frac{\mathcal{V}}{g} \bar{\Delta} \Delta - T \sum_{n,k} \ln[(-i\omega_n + \xi_{e,k+q/2})(-i\omega_n - \xi_{h,-k+q/2}) - \bar{\Delta} \Delta] \quad (16)$$

$$= F_0 + \frac{\mathcal{V}}{g} \bar{\Delta} \Delta + T \sum_{l=1}^{\infty} \frac{1}{l!} \sum_{n,k} \frac{1}{(-i\omega_n + \xi_{e,k+q/2})^l (-i\omega_n - \xi_{h,-k+q/2})^l} (\bar{\Delta} \Delta)^l \quad (17)$$

Where  $F_0 = -T \sum_{n,k} \ln[(-i\omega_n + \xi_{e,k+q/2})(-i\omega_n - \xi_{h,-k+q/2})]$  is the free energy of original fermion gases, which one can verify after some simple algebra[3]. Near but slightly below critical temperature,  $|\Delta|/T \ll 1$ , then we can keep the functional to leading relevant order of  $(\bar{\Delta}, \Delta)$  to obtain Ginzburg-Landau free energy functional:

$$F_{GL}[\bar{\Delta}, \Delta] = \alpha(T, q)(\bar{\Delta} \Delta) + \frac{1}{2} \beta(T, q)(\bar{\Delta} \Delta)^2 \quad (18)$$

Where

$$\alpha = \frac{\mathcal{V}}{g} + T \sum_{n,k} \frac{1}{(-i\omega_n + \xi_{e,k+q/2})(-i\omega_n - \xi_{h,-k+q/2})} \quad (19)$$

$$\beta = T \sum_{n,k} \frac{1}{(-i\omega_n + \xi_{e,k+q/2})^2 (-i\omega_n - \xi_{h,-k+q/2})^2} \quad (20)$$

as presented in the main text of the paper. At specific  $q$ ,  $\alpha(T < T_c(q)) < 0$  while  $\alpha(T > T_c) > 0$ , which characterizes the superconducting-like phase transition of the exciton condensate.

### S-III. Kinetic Theory for Frictional Coulomb Drag

When the double-layer system has not transitioned into an exciton condensate, Coulomb drag still exists, which originates from momentum transfer between the layers due to Coulomb interaction and is called frictional drag[6]. Suppose the drag layer is an open circuit, current in drive layer  $j_1$  will induce a voltage  $V_2$  therein(I-V drag), and drag resistivity  $\rho_D = E_2/j_1$  is defined to characterize the strength of the drag. Alternatively, one can short circuit the drag layer, and a current  $j_2$  is induced by  $j_1$ (I-I drag), and drag ratio  $\zeta = j_2/j_1$  is defined in this case. The second scenario corresponds to our case. In steady state, both  $\rho_D$  and  $\zeta$  can be calculated using Boltzmann transport equation[6-8]. Here we present the derivation of  $\rho_D$  and  $\zeta$  and express them with microscopic parameters. Furthermore, we will try to go to the leading non-linear order and argue the onset of nonreciprocal drag in presence of  $\mathcal{P}, \mathcal{T}$  symmetry breaking.

#### Frictional Coulomb drag for fermions with parabolic dispersion

Consider a 2-dimensional double-layer fermion system with  $d$  the layer separation. The dispersion relations are  $\xi_k^{t,b} = \frac{k^2}{2m_{t,b}} - \mu_{t,b}$  for charge carrier fermions in the top(drive) and bottom(drag) layers, respectively. In our case of electron-hole bilayer setup,  $t = e$  &  $b = h$ , where  $e$  represents electron and  $h$  represents hole. Yet we keep the following derivations general and apply the final formulae to our setup eventually. Denote  $f_0(\xi) = (e^{\beta\xi} + 1)^{-1}$  as the Fermi-Dirac distribution, and  $\tilde{f}_0(\xi) = 1 - f_0(\xi) = f_0(-\xi)$ . We denote  $e_1, e_2$  as charge of carriers in top and bottom layers, respectively. Focusing on the drag layer, in a homogeneous steady state, the Boltzmann equation reads:

$$e_2 \mathbf{E}_2 \cdot \partial_{k_2} f(k_2) = \left( \frac{\partial f(k_2)}{\partial t} \right)_{drag} + \left( \frac{\partial f(k_2)}{\partial t} \right)_{relaxation} \quad (21)$$

For simplicity, we use  $k_1, k_2$  to label momenta of particles in drive and drag layer respectively, and denote  $f(k_1) = f(\xi_{k_1}^t), f(k_2) = f(\xi_{k_2}^b)$ . For I-V drag,  $(\frac{\partial f(k_2)}{\partial t})_{relaxation} = 0$  since bulk of drag layer is in equilibrium; for I-I drag,  $\mathbf{E}_2 = 0$  due to short circuit condition. Since the I-V drag is studied extensively in literature[7, 8], we focus on the I-I drag. In the steady state of I-I drag, the two layers are both carrying current though spatially homogeneous, so we use drifting solution

$$f(k_1) = f_0(k_1) - m_t \mathbf{v}_1 \cdot \partial_{k_1} f_0(k_1) \approx f_0(k_1 - m_t \mathbf{v}_1) \quad (22)$$

$$f(k_2) = f_0(k_2) - m_b \mathbf{v}_2 \cdot \partial_{k_2} f_0(k_2) \approx f_0(k_2 - m_b \mathbf{v}_2) \quad (23)$$

Where  $v_i$  are drift velocity for either layer and  $j_i = n_i e_i v_i$ ,  $i = 1, 2$ . Then the relaxation term in drag layer can be captured by quasi-particle lifetime  $\tau_2$ :

$$\left( \frac{\partial f(k_2)}{\partial t} \right)_{relaxation} = - \frac{f(k_2) - f_0(k_2)}{\tau_2} = \frac{m_b \mathbf{v}_2 \cdot \partial_{k_2} f_0(k_2)}{\tau_2} \quad (24)$$

The drag term originates from interlayer scattering events and can be expressed as:

$$\begin{aligned} \left( \frac{\partial f(k_2)}{\partial t} \right)_{drag} &= - \int \frac{d^2 q}{(2\pi)^2} \int \frac{d^2 k_1}{(2\pi)^2} \mathcal{A}(q) (f(k_1) \tilde{f}(k_1 - q) f(k_2) \tilde{f}(k_2 + q) - f(k_1 - q) \tilde{f}(k_1) f(k_2 + q) \tilde{f}(k_2)) \\ &\times \delta(\xi_{k_1}^t + \xi_{k_2}^b - \xi_{k_1-q}^t - \xi_{k_2+q}^b) \end{aligned} \quad (25)$$

Where  $\mathcal{A}(q) = 2\pi|U(q)|^2$  according to Fermi's golden rule, and  $U(q)$  is matrix element of the screened interlayer Coulomb interaction as discussed in the main text. Now multiply both sides of (21) with  $\mathbf{k}_2$  and integrate over  $\mathbf{k}_2$ , namely apply  $\int \frac{d^2 k_2}{(2\pi)^2} \mathbf{k}_2$  to both sides, obtaining:

$$0 = - \int \frac{d^2 k_2}{(2\pi)^2} \mathbf{k}_2 \frac{f_0(k_2 - m_b \mathbf{v}_2) - f_0(k_2)}{\tau_2} + \int \frac{d^2 k_2}{(2\pi)^2} \mathbf{k}_2 \left( \frac{\partial f(k_2)}{\partial t} \right)_{drag} \quad (26)$$

$$= -n_2 \frac{m_b}{\tau_2} \mathbf{v}_2 + \int \frac{d^2 k_2}{(2\pi)^2} \mathbf{k}_2 \left( \frac{\partial f(k_2)}{\partial t} \right)_{drag} \quad (27)$$

$n_1, n_2$  are carrier densities in top and bottom layers, respectively. The above equation is literally a force balance condition on average — in drag layer, drag force  $F_{drag}$  exerted by drive layer is balanced with frictional force  $\mathbf{f} =$

$-\frac{m_b}{\tau_2} \mathbf{v}_2$ , namely:

$$n_2 \left( -\frac{m_b}{\tau_2} \mathbf{v}_2 + \mathbf{F}_{drag}(\mathbf{v}_1, \mathbf{v}_2) \right) = 0 \quad (28)$$

Where

$$n_2 \mathbf{F}_{drag}(\mathbf{v}_1, \mathbf{v}_2) = \int \frac{d^2 k_2}{(2\pi)^2} \mathbf{k}_2 \left( \frac{\partial f(k_2)}{\partial t} \right)_{drag} \quad (29)$$

$$= - \int \frac{d^2 k_2}{(2\pi)^2} \mathbf{k}_2 \int \frac{d^2 q}{(2\pi)^2} \int \frac{d^2 k_1}{(2\pi)^2} \mathcal{A}(q) (f(k_1) \tilde{f}(k_1 - q) f(k_2) \tilde{f}(k_2 + q) - f(k_1 - q) \tilde{f}(k_1) f(k_2 + q) \tilde{f}(k_2)) \delta(\xi_{k_1}^t + \xi_{k_2}^b - \xi_{k_1-q}^t - \xi_{k_2+q}^b) \quad (30)$$

$$= - \int \frac{d^2 k_2}{(2\pi)^2} \frac{1}{2} (\mathbf{k}_2 - (\mathbf{k}_2 + \mathbf{q})) \int \frac{d^2 q}{(2\pi)^2} \int \frac{d^2 k_1}{(2\pi)^2} \mathcal{A}(q) (f(k_1) \tilde{f}(k_1 - q) f(k_2) \tilde{f}(k_2 + q) - f(k_1 - q) \tilde{f}(k_1) f(k_2 + q) \tilde{f}(k_2)) \delta(\xi_{k_1}^t + \xi_{k_2}^b - \xi_{k_1-q}^t - \xi_{k_2+q}^b) \quad (31)$$

$$= \frac{1}{2} \int \frac{d^2 q}{(2\pi)^2} \mathbf{q} \mathcal{A}(q) \int \frac{d^2 k_1}{(2\pi)^2} \int \frac{d^2 k_2}{(2\pi)^2} (f(k_1) \tilde{f}(k_1 - q) f(k_2) \tilde{f}(k_2 + q) - f(k_1 - q) \tilde{f}(k_1) f(k_2 + q) \tilde{f}(k_2)) \delta(\xi_{k_1}^t + \xi_{k_2}^b - \xi_{k_1-q}^t - \xi_{k_2+q}^b) \quad (32)$$

The substitution  $k_2 \rightarrow (k_2 - (k_2 + q))/2$  only holds when  $f(k_2) = f(-k_2)$  symmetry is preserved. Denote group velocity  $\mathbf{v}(k_{1,2}) = \partial_{k_{1,2}} \xi_{k_{1,2}}^{t,b}$ , we can further express (22), (23) as:

$$f(k_1) = f_0(k_1)(1 + \beta m_t \mathbf{v}_1 \cdot \mathbf{v}(k_1) \tilde{f}_0(k_1)) = f_0(k_1)(1 + \beta \mathbf{v}_1 \cdot \mathbf{k}_1 \tilde{f}_0(k_1)) \quad (33)$$

$$f(k_2) = f_0(k_2)(1 + \beta m_b \mathbf{v}_2 \cdot \mathbf{v}(k_2) f_0(k_2)) = f_0(k_2)(1 + \beta \mathbf{v}_2 \cdot \mathbf{k}_2 f_0(k_2)) \quad (34)$$

Along with detailed balance condition:

$$f_0(\epsilon_1) \tilde{f}_0(\epsilon_2) f_0(\epsilon_3) \tilde{f}_0(\epsilon_4) = f_0(\epsilon_2) \tilde{f}_0(\epsilon_1) f_0(\epsilon_4) \tilde{f}_0(\epsilon_3) \quad \text{if } \epsilon_1 + \epsilon_3 = \epsilon_2 + \epsilon_4 \quad (35)$$

(32) can be further expressed as:

$$\begin{aligned} n_2 \mathbf{F}_{drag}(\mathbf{v}_1, \mathbf{v}_2) &= \frac{1}{2} \int \frac{d^2 q}{(2\pi)^2} \mathbf{q} \mathcal{A}(q) \int \frac{d^2 k_1}{(2\pi)^2} \int \frac{d^2 k_2}{(2\pi)^2} f_0(k_1) \tilde{f}_0(k_1 - q) f_0(k_2) \tilde{f}_0(k_2 + q) [(1 + \beta \mathbf{v}_1 \cdot \mathbf{k}_1 \tilde{f}_0(k_1)) \\ &\quad \times (1 - \beta \mathbf{v}_1 \cdot (\mathbf{k}_1 - \mathbf{q}) f_0(k_1 - q)) (1 + \beta \mathbf{v}_2 \cdot \mathbf{k}_2 \tilde{f}_0(k_2)) (1 - \beta \mathbf{v}_2 \cdot (\mathbf{k}_2 + \mathbf{q}) f_0(k_2 + q)) \\ &\quad - (1 + \beta \mathbf{v}_1 \cdot (\mathbf{k}_1 - \mathbf{q}) \tilde{f}_0(k_1 - q)) (1 - \beta \mathbf{v}_1 \cdot \mathbf{k}_1 f_0(k_1)) (1 + \beta \mathbf{v}_2 \cdot (\mathbf{k}_2 + \mathbf{q}) \tilde{f}_0(k_2 + q)) \\ &\quad \times (1 - \beta \mathbf{v}_2 \cdot \mathbf{k}_2 f_0(k_2))] \delta(\xi_{k_1}^t + \xi_{k_2}^b - \xi_{k_1-q}^t - \xi_{k_2+q}^b) \end{aligned} \quad (36)$$

From (36), we can expand the drag force to both linear and quadratic order with respect to  $v_1, v_2$ , namely  $j_1, j_2$ . Without loss of generality, suppose the drag is in  $x$  direction, at linear order we obtain:

$$F_{drag}(v_1, v_2) = \frac{m_t}{\tau_{D1}} v_1 - \frac{m_b}{\tau_{D2}} v_2 = \gamma_D (v_1 - v_2) \quad (37)$$

Where

$$\gamma_D = \frac{\beta}{16\pi^2 n_2} \int \frac{d^2 q}{(2\pi)^2} |q|^2 \mathcal{A}(q) \int d\omega \frac{\Im \chi_1(q, \omega) \Im \chi_2(q, \omega)}{\sinh^2(\beta\omega/2)} \quad (38)$$

$$\frac{1}{\tau_{D1}} = \frac{\gamma_D}{m_t}, \quad \frac{1}{\tau_{D2}} = \frac{\gamma_D}{m_b} \quad (39)$$

When the dispersions are parabolic, velocities have the exact meaning as parameters of the Galilean boost. Hence  $F_{drag}(v_1, v_2) = F_{drag}(v_1 - v_2)$  and vanishes when  $v_1 = v_2$ , which ensures the vanishing of drag force in absence of relative motion.  $\chi_{1,2}(q, \omega) = - \int \frac{d^2 k}{(2\pi)^2} \frac{f_0(\xi_k^{t,b}) - f_0(\xi_{k+q}^{t,b})}{\omega - \xi_k^{t,b} + \xi_{k+q}^{t,b} + i0^+}$  are susceptibilities of the fermion gases.

Combine (28) and (37), at linear order, we identify the drag ratio

$$\zeta = \frac{v_2}{v_1} = \frac{1}{1 + \tau_{D2}/\tau_2} \quad (40)$$

One can expand (36) to quadratic order, and find that all quadratic terms vanish! Symmetry arguments imply the vanishing before calculation: quadratic terms lead to nonreciprocal drag effect, which has no chance to exist since our fermion dispersions are both isotropic. When anisotropy is introduced in fermion dispersions, one would expect non-vanishing quadratic-order terms, which will be discussed subsequently.

#### Frictional Coulomb drag with general drive layer dispersion

Now suppose the drive layer doesn't have perfect parabolic fermion dispersion any more, e.g. the lower branch in (3):  $\xi_k^t = \frac{k^2}{2m_e} - \lambda \sqrt{(k_x + B/\lambda)^2 + k_y^2 + J^2} - (\mu - \frac{\delta}{2})$ , which breaks both inversion and time reversal symmetry. Suppose the drag layer still has parabolic dispersion in order to use the trick in (32), and without loss of generality we perform the drag experiment in x direction, a similar derivation leads to the result:

$$\begin{aligned} n_2 F_{drag}(v_1, v_2) = & \frac{1}{2} \int \frac{d^2 k_1}{(2\pi)^2} \int \frac{d^2 k_2}{(2\pi)^2} \int \frac{d^2 q}{(2\pi)^2} q_x \mathcal{A}(q) f_0(k_1) \tilde{f}_0(k_1 - q) f_0(k_2) \tilde{f}_0(k_2 + q) [(1 + \beta \bar{m}_t^x v_1 v_x(k_1) \tilde{f}_0(k_1)) \\ & \times (1 - \beta \bar{m}_t^x v_1 v_x(k_1 - q) f_0(k_1 - q)) (1 + \beta v_2 k_{2x} \tilde{f}_0(k_2)) (1 - \beta v_2 (k_{2x} + q_x) f_0(k_2 + q)) \\ & - (1 + \beta \bar{m}_t^x v_1 v_x(k_1 - q) \tilde{f}_0(k_1 - q)) (1 - \beta \bar{m}_t^x v_1 v_x(k_1) f_0(k_1)) (1 + \beta v_2 (k_{2x} + q_x) \tilde{f}_0(k_2 + q)) \\ & \times (1 - \beta v_2 k_{2x} f_0(k_2))] \delta(\xi_{k_1}^t + \xi_{k_2}^b - \xi_{k_1 - q}^t - \xi_{k_2 + q}^b) \end{aligned} \quad (41)$$

Where  $(1/\bar{m}_t^x) = (n_1)^{-1} \int \frac{d^2 k_1}{(2\pi)^2} \partial_{k_{1x}}^2 \xi_{k_1}^t f_0(k_1)$  is the average effective mass. To the quadratic order of  $v_1, v_2$ , we obtain

$$F_{drag}(v_1, v_2) = \frac{\bar{m}_t^x}{\tau_{D1}} v_1 - \frac{m_b}{\tau_{D2}} v_2 + \kappa_{11} v_1^2 + \kappa_{12} v_1 v_2 + \kappa_{22} v_2^2 \quad (42)$$

Where

$$\begin{aligned} \frac{1}{\tau_{D1}} = & \frac{\beta}{8\pi n_2} \int \frac{d^2 q}{(2\pi)^2} \int d\omega \int \frac{d^2 k_1}{(2\pi)^2} q_x (v_x(k_1) - v_x(k_1 - q)) \mathcal{A}(q) (f_0(k_1 - q) - f_0(k_1)) \\ & \times \delta(\omega - \xi_{k_1}^t + \xi_{k_1 - q}^t) \frac{\Im \chi_2(q, \omega)}{\sinh^2(\beta\omega/2)} \end{aligned} \quad (43)$$

$$\begin{aligned} \frac{1}{\tau_{D2}} = & \frac{\beta}{8\pi n_2} \int \frac{d^2 q}{(2\pi)^2} \int d\omega \int \frac{d^2 k_2}{(2\pi)^2} q_x (v_x(k_2 + q) - v_x(k_2)) \mathcal{A}(q) (f_0(k_2) - f_0(k_2 + q)) \\ & \times \delta(\omega + \xi_{k_2}^b - \xi_{k_2 + q}^b) \frac{\Im \chi_1(q, \omega)}{\sinh^2(\beta\omega/2)} \end{aligned} \quad (44)$$

$$= \frac{1}{m_b} \frac{\beta}{16\pi^2 n_2} \int \frac{d^2 q}{(2\pi)^2} |q|^2 \mathcal{A}(q) \int d\omega \frac{\Im \chi_1(q, \omega) \Im \chi_2(q, \omega)}{\sinh^2(\beta\omega/2)} \quad (45)$$

$$\begin{aligned} \kappa_{11} = & -\frac{(\beta \bar{m}_t^x)^2}{16\pi n_2} \int \frac{d^2 q}{(2\pi)^2} \int d\omega \int \frac{d^2 k_1}{(2\pi)^2} q_x \mathcal{A}(q) v_x(k_1 - q) v_x(k_1) (f_0(k_1) - f_0(k_1 - q))^2 \\ & \times \delta(\omega - \xi_{k_1}^t + \xi_{k_1 - q}^t) \frac{\Im(\chi_2(q, \omega) - \chi_2(-q, -\omega))}{\sinh^2(\beta\omega/2)} \end{aligned} \quad (46)$$

$$\begin{aligned} \kappa_{12} = & \frac{\beta^2 \bar{m}_t^x m_b}{2n_2} \int \frac{d^2 q}{(2\pi)^2} \int \frac{d^2 k_1}{(2\pi)^2} \int \frac{d^2 k_2}{(2\pi)^2} q_x \mathcal{A}(q) f_0(k_1) \tilde{f}_0(k_1 - q) f_0(k_2) \tilde{f}_0(k_2 + q) \delta(\xi_{k_1}^t \\ & + \xi_{k_2}^b - \xi_{k_1 - q}^t - \xi_{k_2 + q}^b) [v_x(k_1) v_x(k_2) (1 - f_0(k_1) f_0(k_2)) - v_x(k_1 - q) v_x(k_2 + q) \\ & \times (1 - f_0(k_1 - q) f_0(k_2 + q)) + v_x(k_1) v_x(k_2 + q) (f_0(k_1) - f_0(k_2 + q)) \\ & - v_x(k_1 - q) v_x(k_2) (f_0(k_1 - q) - f_0(k_2))] \end{aligned} \quad (47)$$

$$\begin{aligned}\kappa_{22} = & -\frac{(\beta m_b)^2}{16\pi n_2} \int \frac{d^2q}{(2\pi)^2} \int d\omega \int \frac{d^2k_2}{(2\pi)^2} q_x \mathcal{A}(q) v_x(k_2) v_x(k_2 + q) (f_0(k_2) - f_0(k_2 + q))^2 \\ & \times \delta(\omega + \xi_{k_2}^b - \xi_{k_2+q}^b) \frac{\Im(\chi_1(q, \omega) - \chi_1(-q, -\omega))}{\sinh^2(\beta\omega/2)}\end{aligned}\quad (48)$$

It is evident that when  $\xi_k^t = \xi_{-k}^t$ ,  $\kappa_{22} = 0$ ; when  $\xi_k^b = \xi_{-k}^b$ ,  $\kappa_{11} = 0$ . When both previous symmetry conditions hold,  $\kappa_{12} = 0$  as well, hence all quadratic order terms vanish, forbidding nonreciprocal drag. In our case,  $\kappa_{11} = 0$ , though the rest don't necessarily vanish. The non-vanishing of  $\kappa_{12}, \kappa_{22}$  leads to nonreciprocal Coulomb drag.

Combine (42) and (28), we obtain the following equation:

$$\frac{\bar{m}_t^x}{\tau_{D1}} v_1 - \frac{m_b}{\tau_{D2}} v_2 + \kappa_{11} v_1^2 + \kappa_{12} v_1 v_2 + \kappa_{22} v_2^2 - \frac{m_b}{\tau_2} v_2 = 0 \quad (49)$$

Where  $\kappa_{11} = 0$  is our case. Noticing the typical smallness of  $v_2/v_1$  in frictional drag regime, we keep nonlinear terms in the equation to the leading order of  $v_2/v_1$  and obtain

$$\frac{v_2}{v_1} = \frac{\bar{m}_t^x/\tau_{D1} + \kappa_{11} v_1 + \kappa_{12} v_2}{m_b(1/\tau_2 + 1/\tau_{D2}) + \kappa_{22} v_2} \quad (50)$$

$$\approx \frac{\bar{m}_t^x}{m_b(\tau_{D1}/\tau_2 + \tau_{D1}/\tau_{D2})} + \left( \frac{\kappa_{12}\tau_{D1}}{m_b} - \frac{\kappa_{22}\tau_{D1}(\bar{m}_t^x + \kappa_{11}\tau_{D1}v_1)}{m_b^2} \right) v_2 \quad (51)$$

$$\approx \frac{\bar{m}_t^x}{m_b(\tau_{D1}/\tau_2 + \tau_{D1}/\tau_{D2})} [1 + \left( \frac{\kappa_{12}\tau_{D1}}{m_b} - \frac{\kappa_{22}\tau_{D1}\bar{m}_t^x}{m_b^2} \right) v_1] \quad (52)$$

Namely, up to next leading order, drag ratio  $\zeta = \zeta^{(0)} + \zeta^{(1)}(v_1)$  is a function of  $v_1$ , where

$$\zeta^{(0)} = \frac{n_2 e_2}{n_1 e_1} \frac{\bar{m}_t^x}{m_b(\tau_{D1}/\tau_2 + \tau_{D1}/\tau_{D2})} \quad (53)$$

$$\zeta^{(1)}(v_1) = \zeta^{(0)} \left( \frac{\kappa_{12}\tau_{D1}}{m_b} - \frac{\kappa_{22}\tau_{D1}\bar{m}_t^x}{m_b^2} \right) v_1 \quad (54)$$

The nonzero  $\zeta^{(1)}(v_1)$  term is responsible for both nonlinear and nonreciprocal drag effects.

### Application to electron-hole bilayer

In the electron-hole bilayer setup where  $\xi_k^{t(b)} = \xi_{e(h),k} = \frac{k^2}{2m_{e(h)}} - \mu_{e(h)} - |\lambda_{e(h)}| \sqrt{(k_x + \frac{B}{\lambda_{e(h)}})^2 + k_y^2 + (\frac{J}{\lambda_{e(h)}})^2}$ , which is extensively discussed in the main text. We have

$$\zeta = \frac{I_{\text{drag}}}{I_{\text{drive}}} = \zeta^{(0)} + \zeta^{(1)}(j_{\text{drive}}) \quad (55)$$

Note  $I_{\text{drive,drag}} = j_{\text{drive,drag}} \cdot L_y$ , where  $L_y$  is the effective length of the sample in  $y$  direction, which plays the role of the 1-dimensional cross section of a 2-dimensional sample.

$$\zeta^{(0)} = -\frac{n_h \bar{m}_e^x}{n_e m_h} \frac{1}{\tau_{D1}/\tau_b + \tau_{D1}/\tau_{D2}} \quad (56)$$

$$\zeta^{(1)} = -\zeta^{(0)} \left( \frac{\kappa_{12}\tau_{D1}}{m_h} - \frac{\kappa_{22}\tau_{D1}\bar{m}_e^x}{m_h^2} \right) \frac{j_{\text{drive}}}{n_e e} \quad (57)$$

Where now

$$\begin{aligned}\frac{1}{\tau_{D1}} = & \frac{\beta}{8\pi n_h} \int \frac{d^2q}{(2\pi)^2} \int d\omega \int \frac{d^2k}{(2\pi)^2} q_x (v_x^e(k) - v_x^e(k - q)) \mathcal{A}(q) (f_0(\xi_{e,k-q}) - f_0(\xi_{e,k})) \\ & \times \delta(\omega - \xi_{e,k_1} + \xi_{e,k_1-q}) \frac{\Im\chi_h(q, \omega)}{\sinh^2(\beta\omega/2)}\end{aligned}\quad (58)$$

$$\begin{aligned} \frac{1}{\tau_{D2}} &= \frac{\beta}{8\pi n_h} \int \frac{d^2 q}{(2\pi)^2} \int d\omega \int \frac{d^2 k}{(2\pi)^2} q_x (v_x^h(k+q) - v_x^h(k)) \mathcal{A}(q) (f_0(\xi_{h,k}) - f_0(\xi_{h,k+q})) \\ &\times \delta(\omega + \xi_{h,k} - \xi_{h,k+q}) \frac{\Im \chi_e(q, \omega)}{\sinh^2(\beta\omega/2)} \end{aligned} \quad (59)$$

$$= \frac{1}{m_h} \frac{\beta}{16\pi^2 n_h} \int \frac{d^2 q}{(2\pi)^2} |q|^2 \mathcal{A}(q) \int d\omega \frac{\Im \chi_e(q, \omega) \Im \chi_h(q, \omega)}{\sinh^2(\beta\omega/2)} \quad (60)$$

$$\begin{aligned} \kappa_{12} &= \frac{\beta^2 \bar{m}_e^x m_h}{2n_h} \int \frac{d^2 q}{(2\pi)^2} \int \frac{d^2 k_1}{(2\pi)^2} \int \frac{d^2 k_2}{(2\pi)^2} q_x \mathcal{A}(q) f_0(\xi_{e,k_1}) \tilde{f}_0(\xi_{e,k_1-q}) f_0(\xi_{h,k_2}) \tilde{f}_0(\xi_{h,k_2+q}) \delta(\xi_{e,k_1} \\ &+ \xi_{h,k_2} - \xi_{e,k_1-q} - \xi_{h,k_2+q}) [v_x^e(k_1) v_x^h(k_2) (1 - f_0(\xi_{e,k_1}) f_0(\xi_{h,k_2})) - v_x^e(k_1-q) v_x^h(k_2+q) \\ &\times (1 - f_0(\xi_{e,k_1-q}) f_0(\xi_{h,k_2+q})) + v_x^e(k_1) v_x^h(k_2+q) (f_0(\xi_{e,k_1}) - f_0(\xi_{h,k_2+q})) \\ &- v_x^e(k_1-q) v_x^h(k_2) (f_0(\xi_{e,k_1-q}) - f_0(\xi_{h,k_2}))] \end{aligned} \quad (61)$$

$$\begin{aligned} \kappa_{22} &= -\frac{(\beta m_h)^2}{16\pi n_h} \int \frac{d^2 q}{(2\pi)^2} \int d\omega \int \frac{d^2 k}{(2\pi)^2} q_x \mathcal{A}(q) v_x^h(k) v_x^h(k_2) (f_0(\xi_{h,k}) - f_0(\xi_{h,k+q}))^2 \\ &\times \delta(\omega + \xi_{h,k} - \xi_{h,k+q}) \frac{\Im(\chi_e(q, \omega) - \chi_e(-q, -\omega))}{\sinh^2(\beta\omega/2)} \end{aligned} \quad (62)$$

As what has been discussed previously, nonreciprocal frictional Coulomb drag comes from  $\zeta^{(1)}$  term. Yet when  $\xi_{e,k} = \xi_{e,-k}$ , both  $\kappa_{12}$  and  $\kappa_{22}$  will vanish, which will make  $\zeta^{(1)}$  term vanish. If  $\xi_{e,k} \neq \xi_{e,-k}$  as in our model, nonreciprocal frictional drag is present in general.

---

\* qingdong.jiang@sjtu.edu.cn

- [1] A.-Y. Lu, H. Zhu, J. Xiao, C.-P. Chuu, Y. Han, M.-H. Chiu, C.-C. Cheng, C.-W. Yang, K.-H. Wei, Y. Yang, *et al.*, Janus monolayers of transition metal dichalcogenides, *Nature nanotechnology* **12**, 744 (2017).
- [2] X. Tang and L. Kou, 2d janus transition metal dichalcogenides: Properties and applications, *physica status solidi (b)* **259**, 2100562 (2022).
- [3] A. Altland and B. D. Simons, *Condensed matter field theory* (Cambridge university press, 2010).
- [4] H. Kleinert, Collective quantum fields, *Fortschritte der Physik* **26**, 565 (1978).
- [5] M. Laine and A. Vuorinen, Basics of thermal field theory, *Lect. Notes Phys* **925**, 1701 (2016).
- [6] B. Narozhny and A. Levchenko, Coulomb drag, *Reviews of Modern Physics* **88**, 025003 (2016).
- [7] A.-P. Jauho and H. Smith, Coulomb drag between parallel two-dimensional electron systems, *Physical Review B* **47**, 4420 (1993).
- [8] A. G. Rojo, Electron-drag effects in coupled electron systems, *Journal of Physics: Condensed Matter* **11**, R31 (1999).